Applied Mathematics Letters 166 (2025) 109542

Contents lists available at ScienceDirect

Applied Mathematics Letters

journal homepage: www.elsevier.com/locate/aml

Regular article

Computational analysis of a normalized time-fractional Fisher equation

Soobin Kwak [a], Yunjae Nam [b], Seungyoon Kang [a], Junseok Kim [a,*]

[a] Department of Mathematics, Korea University, Seoul 02841, Republic of Korea
[b] Program in Actuarial Science and Financial Engineering, Korea University, Seoul 02841, Republic of Korea

ARTICLE INFO

Keywords:
Fisher equation
Finite difference scheme
Caputo derivative

ABSTRACT

This study presents a normalized time-fractional Fisher equation to resolve scaling inconsistencies associated with conventional time-fractional derivatives. A finite difference scheme is applied to numerically solve the equation. Computational experiments are conducted to investigate the impact of the fractional order on the system's dynamics. The numerical results demonstrate the influence of memory effects on the solution's evolution and highlight the advantages of the proposed normalization approach for fractional-order models.

1. Introduction

The Fisher equation is a classical reaction–diffusion equation that has been extensively studied for its traveling wave solutions [1] and applications [2] in ecological modeling. To resolve the scaling inconsistencies related to fractional orders, we present the following normalized time-fractional Fisher equation:

$$\frac{\partial^\alpha u}{\partial t^\alpha} = D\frac{\partial^2 u}{\partial x^2} + \rho(1-u)u, \quad 0 < \alpha < 1, \tag{1}$$

$$u(x,0) = u_0(x), \ x \in \Omega = (L_x, \ R_x), \quad u(L_x,t) = \psi_1(t) \text{ and } u(R_x,t) = \psi_2(t), \ t \geq 0, \tag{2}$$

where the normalized time-fractional derivative [3–5] is defined as follows:

$$\frac{\partial^\alpha u(x,t)}{\partial t^\alpha} = \frac{1-\alpha}{t^{1-\alpha}} \int_0^t \frac{\partial u(x,s)}{\partial s} \frac{ds}{(t-s)^\alpha}, \tag{3}$$

which is similar to the Caputo fractional derivative [6,7] and provides a fair comparison across different fractional orders. The time-fractional Fisher equation can be applied to various challenging and interesting problems in chemistry and biology, such as the population genetics of the neutron and flame spreading models [8]. Furthermore, Alquran et al. [9] validated the outcome using a time-fractional equation to analyze the behavioral pattern of the bird species *Phalacrocorax carbo*. The application is based on abundance data collected from the real-world observations. We provide a brief review of previous studies on numerical schemes for the time-fractional Fisher equation. Gabrick et al. [10] proposed a numerical scheme to solve the fractional reaction–diffusion equation under various kernels, which include singular and non-singular types, and the stability conditions explicitly depend on the kernel. Using Caputo fractional derivatives, Gabrick et al. [11] analyzed the effects of fractional differential operators in time, space, and both variables and demonstrated that the time to reach a steady state is significantly influenced by the fractional order. Majeed

* Corresponding author.
E-mail address: cfdkim@korea.ac.kr (J. Kim).
URL: https://mathematicians.korea.ac.kr/cfdkim (J. Kim).

https://doi.org/10.1016/j.aml.2025.109542
Received 30 December 2024; Received in revised form 2 March 2025; Accepted 2 March 2025
Available online 8 March 2025

et al. [12] proposed a numerical algorithm based on the cubic B-spline finite element method to solve time-fractional Burgers' and Fisher equations using the L1 formula for time discretization and the Crank–Nicolson scheme for spatial interpolation. The numerical results demonstrated the method's effectiveness in solving nonlinear fractional equations, validated by error norm calculations. The Yang transform is an integral transform discovered by Yang [13], which is capable of solving fractional partial differential equations using the homotopy perturbation method developed by He [14]. The Yang transform with the homotopy perturbation technique can find an analytical approximate solution for complicated non-linear fractional partial differential equations [15]. Zidan et al. [16] suggested an analytical technique using the Adomian decomposition technique and homotopy perturbation methodology with the Yang transform to solve the time-fractional Fisher equation. The Sumudu transform iterative method, introduced by Watugala [17], is similar to the Laplace transform. However, its distinguishing feature is that the convergent solution is expressed through a recursive relation.

In the above-mentioned studies, researchers mainly focused on developing methods to solve the traditional time-fractional Fisher equation. However, when we investigate and compare the effects of the fractional order, a problem arises because the integral of the weight function of the time-fractional derivative depends on both time and the fractional order [5]. To resolve this issue, we present a normalized time-fractional Fisher equation based on a normalized weighting function [5], where its integral with respect to time is independent of both time and the fractional order.

This paper is organized as follows. Section 2 describes the numerical method for the time-fractional Fisher equation. Section 3 presents the computational experiments. Section 4 provides the conclusions.

2. Computational solutions

We describe a computational scheme for Eq. (1). Let $\Omega_h = \{x_i | x_i = L_x + (i-1)h,\ i = 1, \dots, N_x\}$ be a discrete domain and h be a space step. Let $u_i^n = u\left(x_i,\ t_n\right)$, where $t_n = (n-1)\Delta t$. We discretize Eq. (3) as

$$\begin{aligned}\frac{\partial^\alpha u(x_i, t_{n+1})}{\partial t^\alpha} &= \frac{1-\alpha}{t_{n+1}^{1-\alpha}} \sum_{m=1}^{n} \int_{t_m}^{t_{m+1}} \frac{\partial u(x_i, s)}{\partial s} \frac{ds}{(t_{n+1}-s)^\alpha} \approx \sum_{m=1}^{n} \frac{1-\alpha}{t_{n+1}^{1-\alpha}} \int_{t_m}^{t_{m+1}} \frac{ds}{(t_{n+1}-s)^\alpha} \frac{u_i^{m+1}-u_i^m}{\Delta t} \\ &= \sum_{m=1}^{n} \frac{(n+1-m)^{1-\alpha} - (n-m)^{1-\alpha}}{n^{1-\alpha}} \frac{u_i^{m+1}-u_i^m}{\Delta t}. \end{aligned} \tag{4}$$

As a result, we derive

$$\sum_{m=1}^{n} w_m^n \frac{u_i^{m+1}-u_i^m}{\Delta t} = D \frac{u_{i-1}^{n+1} - 2u_i^{n+1} + u_{i+1}^{n+1}}{h^2} + \rho(1-u_i^n)u_i^{n+1}, \tag{5}$$

where $w_m^n = [(n+1-m)^{1-\alpha} - (n-m)^{1-\alpha}]/n^{1-\alpha}$. Therefore, Eq. (5) becomes

$$-\frac{D}{h^2}u_{i-1}^{n+1} + \left(\frac{w_n^n}{\Delta t} + \frac{2D}{h^2} - \rho(1-u_i^n)\right)u_i^{n+1} - \frac{D}{h^2}u_{i+1}^{n+1} = \frac{w_n^n}{\Delta t}u_i^n - \sum_{m=1}^{n-1} w_m^n \frac{u_i^{m+1}-u_i^m}{\Delta t}. \tag{6}$$

Eq. (6) can be written as $A\mathbf{u}^{n+1} = \mathbf{g}$, where

$$A = \begin{pmatrix} \frac{w_n^n}{\Delta t} + \frac{2D}{h^2} - \rho(1-u_2^n) & -\frac{D}{h^2} & 0 & \cdots & 0 & 0 \\ -\frac{D}{h^2} & \frac{w_n^n}{\Delta t} + \frac{2D}{h^2} - \rho(1-u_3^n) & -\frac{D}{h^2} & \cdots & 0 & 0 \\ \vdots & \vdots & \vdots & \ddots & \vdots & \vdots \\ 0 & 0 & 0 & \cdots & -\frac{D}{h^2} & \frac{w_n^n}{\Delta t} + \frac{D}{h^2} - \rho(1-u_{N_x-1}) \end{pmatrix},$$

$$\mathbf{u}^{n+1} = \begin{pmatrix} u_2^{n+1} \\ u_3^{n+1} \\ \vdots \\ u_{N_x-1}^{n+1} \end{pmatrix},\ \mathbf{g} = \begin{pmatrix} \frac{w_n^n}{\Delta t}u_2^n - F_2^n + \frac{\psi_1^{n+1}}{h^2} \\ \frac{w_n^n}{\Delta t}u_3^n - F_3^n \\ \vdots \\ \frac{w_n^n}{\Delta t}u_{N_x-1}^n - F_{N_x-1}^n + \frac{\psi_2^{n+1}}{h^2} \end{pmatrix}, \text{ and } F_i^n = \sum_{m=1}^{n-1} w_m^n \frac{u_i^{m+1}-u_i^m}{\Delta t}.$$

We may also apply the Fourier spectral method for the diffusion equation [18].

3. Computational tests

To analyze the effect of α with respect to the initial value of u, we reformulate $u(x,t)$ as an ordinary differential equation in time, specifically as $u(t)$, and rewrite Eq. (5) as follows:

$$\sum_{m=1}^{n} w_m^n \frac{u^{m+1}-u^m}{\Delta t} = \rho(1-u^n)u^n. \tag{7}$$

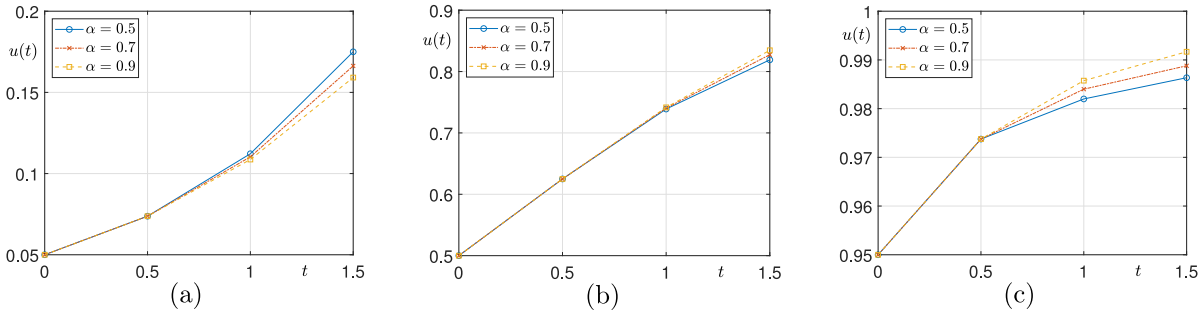

Fig. 1. Temporal evolution of $u(t)$ with $u(0) =$ (a) 0.05, (b) 0.5, and (c) 0.95.

Table 1
The spatial errors and convergence rates.

h	0.20	Rate	0.10	Rate	0.05
Error	1.4056e−02	2.01	3.5001e−03	2.07	8.3493e−04

Table 2
The temporal errors and convergence rates.

Δt	0.20	Rate	0.10	Rate	0.05
Error	6.8668e−01	1.00	3.4347e−01	1.23	1.4595e−01

Eq. (7) can be represented as

$$u^{n+1} = u^n + \frac{\Delta t}{w_n^n}\rho\,(1-u^n)\,u^n - \sum_{m=1}^{n-1} w_m^n \frac{u^{m+1}-u^m}{w_n^n}. \tag{8}$$

Fig. 1 shows the different dynamics for $u(0) = 0.05$, 0.5, and 0.95 with $\Delta t = 0.5$. Fig. 1(a) shows that for a small value of $u(0)$, a smaller value of α results in a greater increase in $u(t)$. On the other hand, as shown in Fig. 1(c), when $u(0)$ is large, a larger value of α has a more significant impact on the growth of $u(t)$.

To verify the order of the numerical scheme used, a convergence test is conducted. Let us consider an initial condition:

$$u(x,0) = \frac{1}{\left(1+e^{x-10}\right)^2}, \qquad \Omega = (0,100). \tag{9}$$

Tables 1 and 2 provide the maximum-norm error $\|u_{\text{ref}} - u\|_\infty$ and rate of the numerical solution for space and time, where u_{ref} denotes the reference solution. The parameters used are $\psi_1(t) = 1$, $\psi_2(t) = 0$, $\alpha = 0.7$, $\rho = 6$, $D = 1$, $\Delta t =$ 1.e−3, a final time $T = 2$. The reference solutions in Tables 1 and 2 were obtained using $h = 0.0125$ and $\Delta t =$ 1.5625.e−4, respectively. When the error with respect to time is investigated, the spatial step size is fixed $h = 0.1$.

We note that this paper focuses on the proposal of a normalized time-fractional Fisher equation and the investigation of fractional-order effects. For the analysis of the numerical scheme, please refer to [19].

To investigate the effect of α, the initial condition (9) is considered in $\Omega = (1,200)$. Here, the used parameters are $\psi_1(t) = 1$, $\psi_2(t) = 0$, $D = 1$, $\rho = 6$, $N_x = 2001$, $\Delta t =$ 2.e−3, and $T = 2.5$. Fig. 2 shows the temporal evolution and final profiles of $u(x,t)$ for different fractional orders α. Fig. 2(a), (b), and (c) show the temporal evolution of the solution $u(x,t)$ for $\alpha = 0.5$, 0.7, and 1, respectively. Fig. 2(d) shows the final time solution of $u(x,T)$ for each value of α, compared to the initial condition $u(x,0)$. As the value of α increases, the evolution speed of $u(x,t)$ becomes slower. However, when observing the overall profile, the case where $\alpha = 1$ represents dynamics similar to a traveling wave solution. For $\alpha \neq 1$, as the value of α decreases, the initial profile near $x = 10$ tends to be preserved.

We investigate the effects of α in more detail. In $\Omega = (0,200)$, the initial condition is given by

$$u(x,0) = \begin{cases} 1, & \text{if } 21 \le x \le 30, \\ \dfrac{1}{\left(1+e^{x-10}\right)^2}, & \text{otherwise.} \end{cases}$$

The following parameter values are used: $\psi_1(t) = 1$, $\psi_2(t) = 0$, $D = 1$, $\rho = 6$, $N_x = 2001$, $T = 2.5$, and $\Delta t =$ 2.e−3. Fig. 3 shows the dynamics of $u(x,t)$ for three different values of the fractional order α. Fig. 3(a), (b) and (c) are the numerical results of $u(x,t)$ with $\alpha = 0.5$, 0.7, and 1, respectively. In Fig. 3(d), we can certainly observe the memory effect of α through the different results of $u(x,T)$ for each α.

We consider the following initial condition with complex perturbation:

$$u(x,0) = 0.05x + 0.05x\cos(\pi x), \qquad \Omega = (0,10),$$

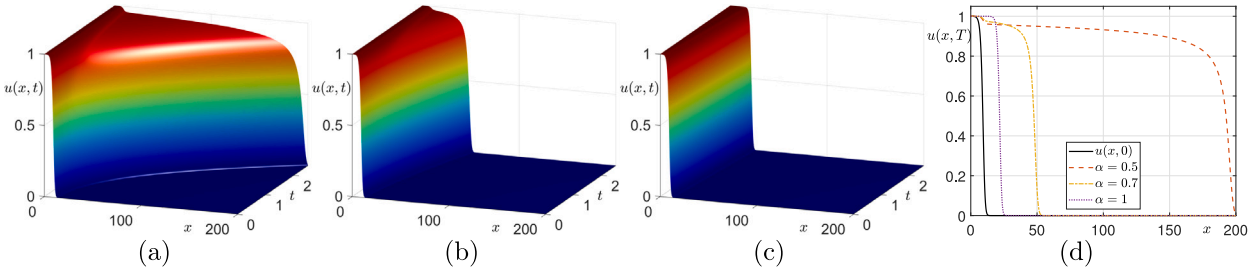

Fig. 2. The temporal evolution of $u(x,t)$ with (a) $\alpha = 0.5$, (b) $\alpha = 0.7$, and (c) $\alpha = 1$. (d) The final time profile of $u(x,T)$ at $T = 2.5$.

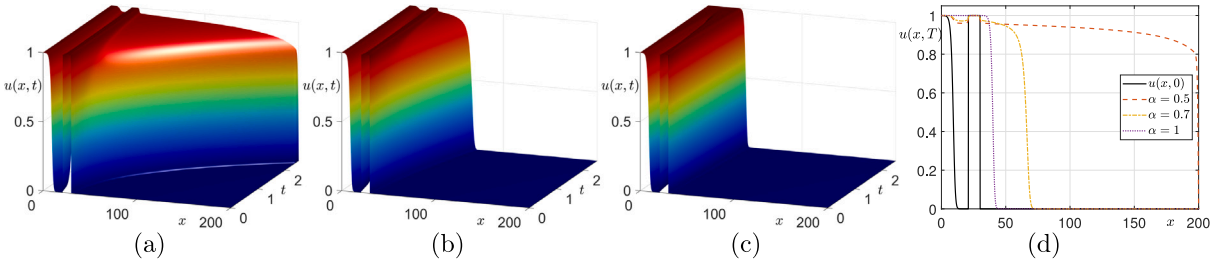

Fig. 3. Mesh plot of $u(x,t)$: (a) $\alpha = 0.5$, (b) $\alpha = 0.7$, and (c) $\alpha = 1$. (d) is the solution of $u(x,T)$ for $\alpha = 0.5$, 0.7, and 1.

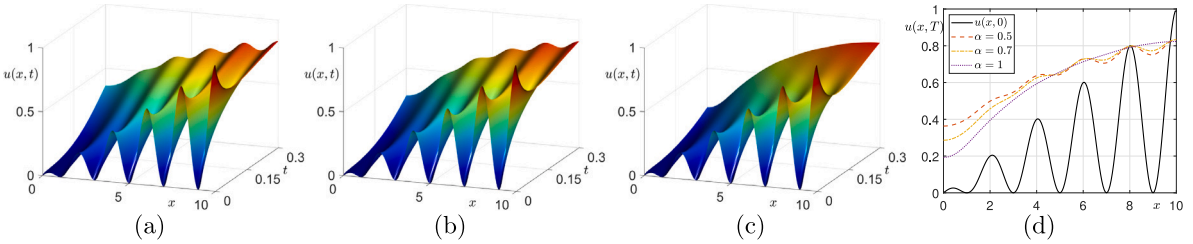

Fig. 4. Dynamics of $u(x,t)$ for different fractional orders: (a) $\alpha = 0.5$, (b) $\alpha = 0.7$, and (c) $\alpha = 1$. (d) shows a comparison of $u(x,T)$ with the initial condition $u(x,0)$.

and investigate the effects of fractional order α when the diffusion coefficient D is large. Here, we consider a no-flux condition. The specific parameter values used are $D = 2$, $\rho = 6$, $\Delta t = 5.\text{e}{-4}$, $T = 0.3$, and $h = 0.05$. Fig. 4(a)–(c) present temporal evolution of $u(x,t)$ as mesh plots for $\alpha = 0.5$, $\alpha = 0.7$, and $\alpha = 1$, respectively. Fig. 4(d) shows the results of $u(x,T)$ for each α value along with the initial condition $u(x,0)$. We observe a strong memory effect, as smaller α values tend to preserve the initial shape despite the large diffusion coefficient.

4. Conclusions

In this paper, we introduced a normalized time-fractional Fisher equation to resolve challenges in analyzing fractional dynamics and provide a more consistent framework for comparing behaviors at different fractional orders. The proposed numerical scheme, based on a finite difference method, was validated through computational experiments, and demonstrated accuracy and efficiency in capturing the dynamics of the system. The numerical results highlighted the influence of fractional orders on growth processes. Future research could further extend this framework to more complex fractional systems and multidimensional domains. For example, the operator splitting method (OSM) can be applied to obtain numerical solutions for the two-dimensional (2D) and three-dimensional (3D) normalized time-fractional Fisher equations. First, the 2D normalized time-fractional Fisher equation is briefly considered.

$$\begin{aligned} \frac{\partial^\alpha u(x,y,t)}{\partial t^\alpha} &= D\left(\frac{\partial^2 u(x,y,t)}{\partial x^2} + \frac{\partial^2 u(x,y,t)}{\partial y^2}\right) + \rho(1-u(x,y,t))u(x,y,t),\ (x,\ y) \in \Omega,\ t > 0, \\ u(x,y,0) &= u_0(x,y),\ (x,\ y) \in \Omega = (L_x,\ R_x) \times (L_y,\ R_y). \end{aligned} \tag{10}$$

Let $u_{ij}^n = u(x_i, y_j, t_n)$, where $y_j = L_y + (j-1)h$, then Eq. (10) is discretized as follows:

$$\frac{\partial^\alpha u(x_i, y_j, t_{n+1})}{\partial t^\alpha} \approx \sum_{m=1}^{n} \frac{(n+1-m)^{1-\alpha} - (n-m)^{1-\alpha}}{n^{1-\alpha}} \frac{u_{ij}^{m+1} - u_{ij}^m}{\Delta t} = \sum_{m=1}^{n} w_m^n \frac{u_{ij}^{m+1} - u_{ij}^m}{\Delta t}$$
$$= w_n^n \frac{u_{ij}^{n+1} - u_{ij}^n}{\Delta t} + \sum_{m=1}^{n-1} w_m^n \frac{u_{ij}^{m+1} - u_{ij}^m}{\Delta t}.$$

Then, we obtain u_{ij}^{n+1} through the following three steps.

$$Step\ 1: \ \frac{u_{ij}^* - u_{ij}^n}{\Delta t} = \frac{D}{w_n^n}\left(\frac{u_{i-1,j}^* - 2u_{ij}^* + u_{i+1,j}^*}{h^2}\right) - \frac{1}{2}s_{ij}^n.$$

$$Step\ 2: \ \frac{u_{ij}^{**} - u_{ij}^*}{\Delta t} = \frac{D}{w_n^n}\left(\frac{u_{i,j-1}^{**} - 2u_{ij}^{**} + u_{i,j+1}^{**}}{h^2}\right) - \frac{1}{2}s_{ij}^n.$$

$$Step\ 3: \ \frac{u_{ij}^{n+1} - u_{ij}^{**}}{\Delta t} = \frac{\rho(1-u_{ij}^n)u_{ij}^{n+1}}{w_n^n},$$

where $s_{ij}^n = \sum_{m=1}^{n-1} w_m^n (u_{ij}^{m+1} - u_{ij}^m)/(w_n^n \Delta t)$. Further details about the OSM can be found in [20]. For the numerical solution of the 3D normalized time-fractional Fisher equation, it is a straightforward extension of the 2D case. Inevitably, this process increases the computational time. To reduce the computational complexity and CPU time, we can consider a method such as meshless method [21].

Acknowledgments

The corresponding author (J.S. Kim) was supported by the Korea University Grant, Republic of Korea. We thank the reviewers for their time and effort in reviewing our manuscript and for their valuable suggestions.

Data availability

No data was used for the research described in the article.

References

[1] S.W. McCue, M. El-Hachem, M.J. Simpson, Exact sharp-fronted travelling wave solutions of the Fisher–KPP equation, Appl. Math. Lett. 114 (2021) 106918, http://dx.doi.org/10.1016/j.aml.2020.106918.
[2] B. Ju, W. Qu, Three-dimensional application of the meshless generalized finite difference method for solving the extended Fisher–Kolmogorov equation, Appl. Math. Lett. 136 (2023) 108458, http://dx.doi.org/10.1016/j.aml.2022.108458.
[3] K.A. Lazopoulos, A.K. Lazopoulos, Fractional vector calculus and fractional continuum mechanics, Prog. Fract. Differ. Appl. 2 (1) (2016) 67–86, http://dx.doi.org/10.18576/pfda/020202.
[4] M. Jornet, J.J. Nieto, Power-series solution of the L-fractional logistic equation, Appl. Math. Lett. 154 (2024) 109085, http://dx.doi.org/10.1016/j.aml.2024.109085.
[5] C. Lee, Y. Nam, M. Bang, S. Ham, J. Kim, Numerical investigation of the dynamics for a normalized time-fractional diffusion equation, AIMS Math. 9 (2024) 26671–26687, http://dx.doi.org/10.3934/math.20241297.
[6] J. Calatayud, M. Jornet, C.M.A. Pinto, On the interpretation of Caputo fractional compartmental models, Chaos Solitons Fractals 186 (2024) 115263, http://dx.doi.org/10.1016/j.chaos.2024.115263.
[7] L. Qing, X. Li, Analysis of a meshless generalized finite difference method for the time-fractional diffusion-wave equation, Comput. Math. Appl. 172 (2024) 134–151, http://dx.doi.org/10.1016/j.camwa.2024.08.008.
[8] X. Zhang, Liu Juan, An analytic study on time-fractional Fisher equation using homotopy perturbation method, Walailak J. Sci. Tech. 11 (11) (2014) 975–985, http://dx.doi.org/10.14456/WJST.2014.72.
[9] M. Alquran, K. Al-Khaled, T. Sardar, J. Chattopadhyay, Revisited Fisher's equation in a new outlook: a fractional derivative approach, Phys. A Stat. Mech. Appl. 438 (2015) 81–93, http://dx.doi.org/10.1016/j.physa.2015.06.036.
[10] E.C. Gabrick, P.R. Protachevicz, E.K. Lenzi, E. Sayari, J. Trobia, M.K. Lenzi, F.S. Borges, I.L. Caldas, A.M. Batista, Fractional diffusion equation under singular and non-singular kernel and its stability, Fract. Fract. 7 (11) (2023) 792, http://dx.doi.org/10.3390/fractalfract7110792.
[11] E.C. Gabrick, P.R. Protachevicz, D.L. Souza, J. Trobia, E. Sayari, F.S. Borges, E.K. Lenzi, Transient dynamics of a fractional Fisher equation, Fract. Fract. 8 (3) (2024) 143, http://dx.doi.org/10.3390/fractalfract8030143.
[12] A. Majeed, M. Kamran, M.K. Iqbal, D. Baleanu, Solving time fractional Burgers' and Fisher's equations using cubic B-spline approximation method, Adv. Differ. Equ. 2020 (1) (2020) 175, http://dx.doi.org/10.1186/s13662-020-02619-8.
[13] X.J. Yang, A new integral transform method for solving steady heat-transfer problem, Therm. Sci. 20 (2016) 639–642, http://dx.doi.org/10.2298/TSCI16S3639Y.
[14] J.H. He, Homotopy perturbation technique, Comput. Methods Appl. Mech. Engrg. 178 (3–4) (1999) 257–262, http://dx.doi.org/10.1016/S0045-7825(99)00018-3.
[15] T.A.J. Al-Griffi, A.S.J. Al-Saif, Yang transform–homotopy perturbation method for solving a non-Newtonian viscoelastic fluid flow on the turbine disk, ZAMM- Z. Angew. Math. Mech. 102 (8) (2022) e202100116, http://dx.doi.org/10.1002/zamm.202100116.
[16] A.M. Zidan, A. Khan, R. Shah, M.K. Alaoui, W. Weera, Evaluation of time-fractional Fisher's equations with the help of analytical methods, AIMS Math. 7 (10) (2022) 18746–18766, http://dx.doi.org/10.3934/math.20221031.
[17] G.K. Watugala, Sumudu transform: a new integral transform to solve differential equations and control engineering problems, Internat. J. Math. Ed. Sci. Tech. 24 (1) (1993) 35–43, http://dx.doi.org/10.1080/0020739930240105.

[18] S. Ham, S. Kwak, H.G. Lee, Y. Hwang, J. Kim, A maximum principle of the Fourier spectral method for diffusion equations, Electron. Res. Arch. 31 (2023) 5396–5405, http://dx.doi.org/10.3934/era.2023273.
[19] G.H. Gao, H.W. Sun, Z.Z. Sun, Stability and convergence of finite difference schemes for a class of time-fractional sub-diffusion equations based on certain superconvergence, J. Comput. Phys. 280 (2015) 510–528, http://dx.doi.org/10.1016/j.jcp.2014.09.033.
[20] S. Kwak, S. Kang, S. Ham, Y. Hwang, G. Lee, J. Kim, An unconditionally stable difference scheme for the two-dimensional modified Fisher–Kolmogorov–Petrovsky–Piscounov equation, J. Math. 2023 (1) (2023) 5527728, http://dx.doi.org/10.1155/2023/5527728.
[21] L. Qing, X. Li, Meshless analysis of fractional diffusion-wave equations by generalized finite difference method, Appl. Math. Lett. 157 (2024) 109204, http://dx.doi.org/10.1016/j.aml.2024.109204.